Journal of Engineering and Technology for Industrial Applications

ITEGAM-JETIA

Manaus, v.11 n.52, p. 186-195. March./April., 2025.
DOI: https://doi.org/10.5935/jetia. v11i52.1604

ISSN ONLINE: 2447-0228

RESEARCH ARTICLE OPEN ACCESS

COMPARATIVE STUDY OF 2D DESIGNS OF 12/8 AND 10/8 SWITCHED RELUCTANCE MOTORS USING ANSYS MAXWELL

Layachi Chebabhi[1], Toufik tayeb Naas[2], Mohamed Zitouni[3]

[1] Laboratory of Applied Automation and Industrial Diagnostics (LAADI), Department of Mechanical Engineering in the Faculty of Science and Technology, Ziane Achour University of Djelfa, PO Box 3117, Djelfa 17000, Algeria.
[2] Laboratory of Renewable Energy Systems Applications (LASER), Department of Mechanical Engineering in the Faculty of Science and Technology, Ziane Achour University of Djelfa, PO Box 3117, Djelfa 17000, Algeria.
[3] Laboratory of Electrotechnical Research L.R.E, National Polytechnic School (ENP), Department of Electrical Engineering in the Faculty of Science and Technology, Ziane Achour University of Djelfa, PO Box 3117, Djelfa 17000, Algeria.

[1]https://orcid.org/0009-0002-4451-8533, [2]http://orcid.org/0000-0002-5539-6415, [3]https://orcid.org/0009-0003-3088-7431

Email: layachi.chebabhi@univ-djelfa.dz, t.naas@univ-djelfa.dz, med.zitouni@univ-djelfa.dz

ARTICLE INFO

Article History
Received: February 02, 2025
Revised: March 20, 2025
Accepted: March 15, 2025
Published: April 30, 2025

Keywords:
Switched Reluctance Motor,
ANSYS Maxwell,
Operating Conditions,
Electromagnetic Analysis,
Losses.

ABSTRACT

The switched reluctance motor (SRM) is one of the common industrial applications where many fields of different models are used, but they differ in performance, thus the selection of the appropriate prototype must be determined according to the application's requirements. In this study, a comparative analysis was conducted between 12/8 and 10/8 switched reluctance motors (SRMs) using ANSYS Maxwell where the same dimensions, parameters, and operating conditions were adopted in the designs and only the number of stator poles were changed to evaluate the magnetic, mechanical, and electrical characteristics. Then we study their effect on the SRMs performance focusing on several aspects of torque, speed, various losses, electromagnetic analysis of intensity, and magnetic flux density. Electrical losses were reviewed, and the study revealed significant differences between the SRMs' electromagnetic performance, highlighting the importance of the SRM design to reduce losses and improve efficiency. The results show that the importance of choosing between the two SRMs depends on the application requirements, whether it requires high speed and efficiency or high torque. This study provides a comprehensive insight into the SRM designs deep analysis, supporting the drive for more efficient and sustainable technology in optimizing the electric motors' overall performance.

I. INTRODUCTION

During recent years, researchers have focused on enhancing and improving various electric motor prototype models and control techniques [1-3], such as Switched Reluctance Motors (SRMs). SRMs have emerged as a suitable choice for industrial power applications in electric transportation and renewable energy due to their simple structure [4],[5], low cost because of the absence of permanent magnets, high reliability, ability to operate in extreme conditions, and durability. The SRMs function on the principle of magnetic pole excitation, which produces varying torque, which makes the focus on the geometry and the pole design of the rotor and stator crucial in establishing the characteristics and performance of this type of motor.

Despite the features of the SRMs, they have drawbacks that affect their behavior in operation, such as the cogging torque and ripples [6],[7]. The difficulty in controlling speed and torque accurately [8-10]. High noise and vibration due to direct magnetic force variations during operation [11],[12]. Complexity in the design of magnetic coils [13]. Power loss due to eddy currents and thermal losses [14]. Performance fluctuates with variations in speed and sensitivity to changes in load and voltage [15]. Several researchers have been developing prototypes of SRMs for various application requirements of solar water pumping systems [16],[17], electric vehicle EV [18-20], elevator applications [21], and cooling fan applications [22]. Recent research has focused on optimizing the SRMs through Artificial Intelligence and machine learning [23-25]. The selection of the material applied to the stator and rotor in the SRMs contributes to minimizing losses and significantly increasing efficiency [26].

The direct torque control (DTC) method for the 5-phase 10/8 SRMs was introduced, focusing on achieving rapid response torque and precise stator flux control [27], while the same method was proposed based on the Fuzzy method to reduce torque ripples [28]. Multilevel inverters have been investigated by using space vector modulation (SVM) in controlling SRM applications with a focus on 10/8, 8/6 and 6/4 geometric types [29]. A validated analytical model for 10/8 and 8/6 SRM was presented. To prove the accuracy, the results were compared with experimental measurements [30]. A novel SRM that has a permanent magnet between the pole tips of the stator is proposed to enhance efficiency and improve torque compared to traditional SRMs [31].

Various control strategies of the 12/8 switched reluctance motor were compared [32]. A design of 12/8 SRM with a segmental rotor type is proposed for cooling fan applications. The structure rotor consists of a series of discrete segments, and the stator consists of two types of poles: auxiliary and exciting poles [33]. A comparative analysis of winding arrangement types for a 12/8 SRM is presented, focusing on the reduction of flux reversal and analysis of torque performance [34].

The analysis and optimization of a 12/8 SRM using the Grey Wolf Optimization (GWO) algorithm for electric vehicle applications is proposed with a focus on enhancing the torque density through geometric optimizations [35]. The torque performance of 12/8 SRM is enhanced by checking the embrace of rotor poles and focusing on the rotor and stator pole arc to obtain minimum ripple torque and maximum average torque [36]. A study of the magnetic characteristics of three-phase 12/8 SRM is presented to improve the starting torque by focusing on the effect of important geometric parameters on enhancing efficiency and torque [37].

Although previous research has provided many 12/8 and 10/8 SRM designs for electric vehicles and various industrial applications, and while they differ in the number of stator poles only, they are significantly different in behavior in many aspects, therefore it is critical to select the SRM accurately according to the application requirements.

This paper aims to conduct an analytical study to compare the behavior of two SRMs with similar parameters, dimensions and operating conditions, focusing on changing only the number of stator poles to investigate their effect on the SRM's performance in terms of efficiency, losses and electromagnetic behavior. This comparison is based on data from detailed simulation results using ANSYS Maxwell that includes electromagnetic analysis of the magnetic field. As well as analysis of performance curves for efficiency, torque, speed, stranded losses, current, voltage, and flux linkages.

Finally, this research contributes to the field of SRM design optimization by focusing on factors that affect the performance such as pole and core design, magnetic flux distribution, coil resistance improvement, and loss reduction, thereby enhancing the sustainability, operational flexibility, and the performance efficiency of the SRMs in various industrial applications. The results of this detailed analysis provide practical data and indicators to enable the selection of the most suitable 12/8 and 10/8 SRMs based on specific operating conditions. This contributes to the improvement of these motors and their ability to be adapted to different application requirements. The finite element method offers many advantages in simplifying complex geometry models in a fast time, making it a common choice in many fields of electrical engineering.

This paper is structured as follows: in section 2, the proposed designs with their basic dimensions of the 12/8 and 10/8 SRMs. Section 3 presents the finite element method in electrical machines. Section 4 incorporates mathematical modeling of the basic equations for the SRMs. In Section 5, the simulation results and comparison of the SRMs are discussed. Finally, section 6 provides a conclusion and summary of this work.

II. APPROACHED DESIGN OF THE SWITCHED RELUCTANCE MOTORS

This paper provides modeling and designing of 12/8 and 10/8 (Figure 1) switched reluctance motors based on similar proportions and parameters in both motors, as illustrated in Table 1. The stator poles were changed only to examine the effect of increasing stator poles on the performance of the machines. Steel 1008 was applied in addition to copper in the stator and rotor parts because the selected materials contribute to reducing total losses and increasing efficiency [26]. The motors were designed under a voltage of 220 V, speed of 3000 RPM, and power of 5000 W. At first, the basic dimensions and appropriate operating conditions were specified according to various mathematical equations and basic computations. The prototype was created and tested using the ANSYS RMxprt tool to evaluate the essential parameters and verify the initial designs. The efficiency of the obtained machines is estimated to be more than 95 %. After that, two-dimensional models were established using the Maxwell2D tool to compare the performance of the SRMs in terms of efficiency, torque, speed, total losses and various other machine data and performance curves. The ANSYS Maxwell approach is adopted by the finite element method, which is accurate and fast in simplifying complex models.

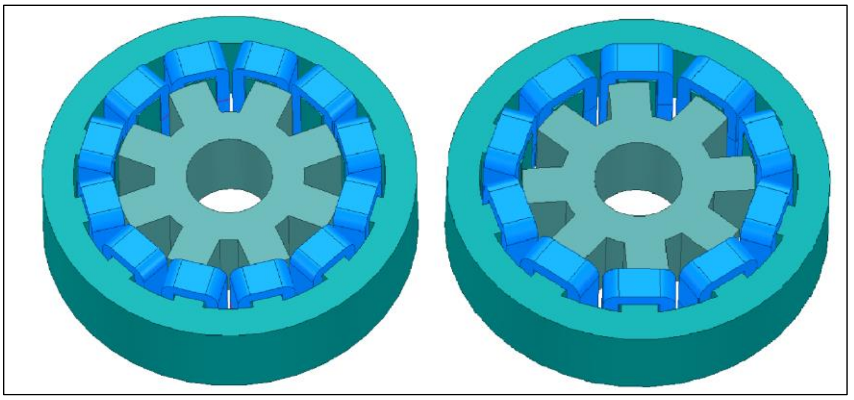

Figure 1: 3D models of the 12/8 and 10/8 SRMs.
Source: Authors, (2025).

Table 1: Parameters of the presented 12/8 and 10/8 SRMs.

Parameters	12/8 SRM	10/8 SRM
Outer Diameter of Stator (mm):	150	150
Inner Diameter of Stator (mm):	95	95
Number of Stator Poles:	12	10
Pole Embrace:	0.6	0.6
Outer Diameter of Rotor (mm):	94	94
Inner Diameter of Rotor (mm):	50	50
Length of Stator Core (mm):	70	70
Type of Steel:	steel_1008	steel_1008
Number of Rotor Poles:	8	8
Pole Embrace:	0.5	0.5
Yoke Thickness (mm):	12	12
Rated Output Power (kW):	5	5
Rated Voltage (V):	220	220
Given Rated Speed (rpm):	3000	3000
Operating Temperature (C):	75	75

Source: Authors, (2025).

Table 2 indicates the copper and steel material consumption in the switched reluctance motors for the rotor and stator parts. The material consumption is similar for both machines in the rotor part, with a slight difference in the weight of copper and steel in the stator core.

Table 2: Materials consumption in the SRMs.

MATERIALS	12/8 SRM	10/8 SRM
Stator Copper Density (kg/m^3):	8900	8900
Stator Core Steel Density (kg/m^3):	7872	7872
Rotor Core Steel Density (kg/m^3):	7872	7872
Stator Copper Weight (kg):	1.25071	1.36846
Stator Core Steel Weight (kg):	4.30679	4.30611
Rotor Core Steel Weight (kg):	2.06099	2.06099
Total Net Weight (kg):	7.61849	7.73556
Stator Core Steel Consumption (kg):	8.42751	8.42751
Rotor Core Steel Consumption (kg):	3.77157	3.77157

Source: Authors, (2025).

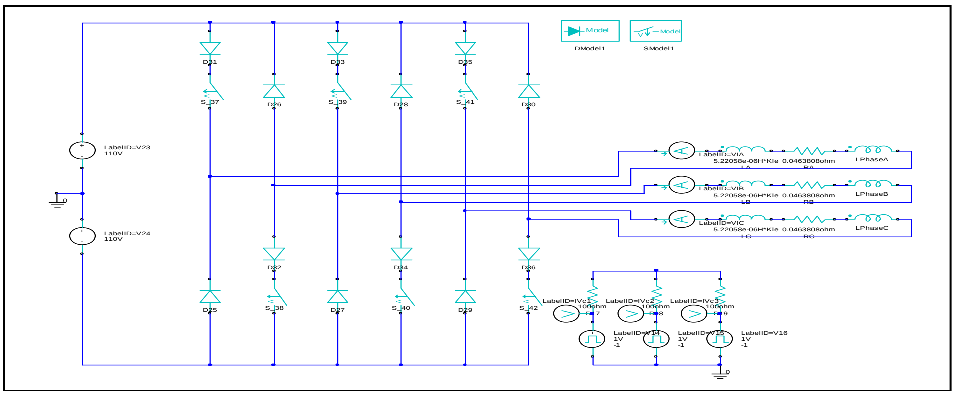

Figure 2: Drive circuit of the 12/8 and 10/8 switched reluctance motors.
Source: Authors, (2025).

III. FINITE ELEMENT METHOD

The finite element method (FEM) is a numerical technique based on dividing a complex geometric field into many small elements to simplify and facilitate its mathematical handling. It is used in solving partial differential equations relating to various physical systems approximately within each element separately after the solutions for all elements are combined to obtain a comprehensive overview of the system's performance. The electromagnetic field distribution of the flux, the vectorial distribution of magnetic flux, and the magnetic intensity in a switched reluctance motor can be solved using the FEM. The electromagnetic analysis of the interaction between the stator and rotor is crucial to ensuring optimal functioning. Both SRMs were designed with the same dimensions and conditions applied except for the number of stator poles changed, as shown in Figure 1 and Table 1.

The Finite Element Method (FEM) is a powerful, accurate and speedy design tool used to enhance many industrial applications designs such as electrical machines and transformers, which contributes to increasing efficiency and reliability, improving overall system performance, and reducing magnetic losses. Electromagnetic analysis based on the ANSYS and FEM allows to specify the parts that are exposed to the magnetic saturation that must be focused on to reduce electrical losses. It permits the evaluation of the interactions between electric currents and magnetic fields in complex components and systems, focusing on the non-linear properties of magnetic materials, the effects of eddy currents and magnetic flux distribution on the performance.

IV. MATHEMATICAL MODELING OF THE SWITCHED RELUCTANCE MOTOR

For a thorough comprehension of the dynamic behavior and determination of the main impacts on a switched reluctance motor's performance, mathematical equations are considered that contribute to illustrating the interrelation between various components such as torque, power, and efficiency. These equations reflect the theoretical underpinnings of electromagnetic analysis and the analysis of experimental data. These later are crucial to explain the transformation of energy, the effect of external load on the motor, and the interactions between magnetic fields and mechanical motion, which contribute to a detailed examination of the complex behavior of the machines under various operating conditions.

From the equivalent circuit given in Figure 3, the phase voltage equation of the SRMs is given in Equation 1:

$$V = iRs + \frac{d\lambda}{dt}(\theta, i) \tag{1}$$

Where i is the phase current, R_s the phase resistance, θ the rotor position, and λ the flux linkage for each phase that is expressed by:

$$\lambda = L(\theta, i)i \tag{2}$$

Where L is the dynamical winding inductance that depends on the rotor position and the current per phase excitation, the equation of voltage for a phase can be defined as:

$$V = iRs + \frac{L(\theta,i)di}{dt} + i\frac{dL}{dt}(\theta,i) \quad (3)$$

$$V = iRs + L(\theta,i)\frac{di}{dt} + i\frac{d\theta}{dt}\frac{dL}{d\theta}(\theta,i) \quad (4)$$

The derivative of the rotor's angular position θ relative to the time is the angular speed of the machine ω_m, then:

$$V = iRs + L(\theta,i)\frac{di}{dt} + i\omega_m\frac{dL}{d\theta}(\theta,i) \quad (5)$$

Where ω_m is the angular speed.

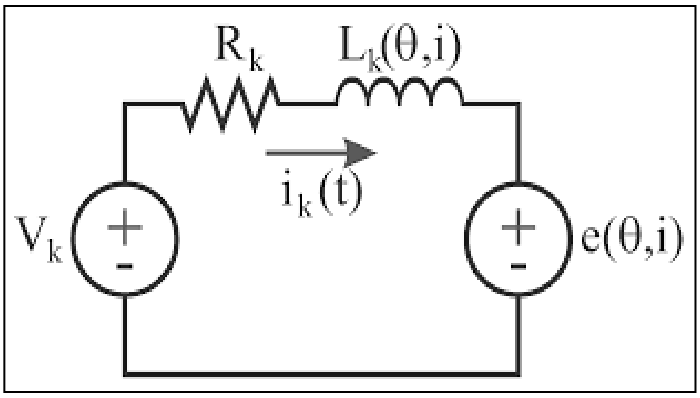

Figure 3: The SRM per phase equivalent circuit.
Soucer: [38].

$$e = -d\varphi(i,\theta)/dt \quad (6)$$

Where $\varphi(i, \theta)$ is the flux linkage that represents a function of the current and the angle of the rotor. Then:

$$\frac{d\varphi(i,\theta)}{dt} = \frac{Ldi}{dt} + \frac{idl}{d\theta}\frac{d\theta}{dt}\frac{Ldi}{dt} + \omega_m i\frac{dl}{d\theta} \quad (7)$$

The switched reluctance motor's amount of power P developed is expressed by Equation 8:

$$P = \frac{Lidi}{dt} + \omega_m i^2\frac{dl}{dt} \quad (8)$$

The SRM energy stored in the magnetic field W_e can be obtained as:

$$We = \frac{1}{2}Li^2 \quad (9)$$

The power generated by the change in the magnetic field is expressed by Equations 10 and 11:

$$\frac{dwe}{dt} = \frac{1}{2}L2i\frac{di}{dt} + \frac{1i^2dL}{2} \quad (10)$$

$$\frac{dWe}{dt} = Li\frac{di}{dt} + \frac{\frac{1}{2}i^2dL}{d\theta}\omega_m \quad (11)$$

Where P_m is the difference between the received power from the supply and the power due to the magnetic field variation and is expressed in Equation 12:

$$P_m = \omega_m T_m \quad (12)$$

$$P_m = \frac{1}{2}\omega_m i^2\frac{dL}{d\theta} \quad (13)$$

The switched reluctance motor air gap power P_{ag} is given as follows in Equations 14 and 15:

$$P_{ag} = \frac{1}{2}\mathrm{i}^2\frac{dL(\theta,i)}{dt} = \frac{1}{2}\mathrm{i}^2\frac{dL(\theta,i)}{d\theta}\frac{d\theta}{dt} \quad (14)$$

$$P_{ag} = \frac{1}{2}\mathrm{i}^2\frac{dL(\theta,i)}{d\theta}\omega_{\mathrm{m}} \quad (15)$$

The main contribution to the developing mechanical power in the rotor is the contribution from the air gap power. The equation for the developed mechanical power of the rotor is provided in Equation 12.

The SRM electromagnetic torque for phases can be calculated by summing the torque of the phases T_{ph}:

$$\begin{aligned} T_{ph} &= \frac{1}{2}i^2\frac{dL(i,\theta)}{d\theta} \\ T_e &= \sum_m T_{ph} \end{aligned} \quad (16)$$

The average torque T_{avg} equation is given as follow:

$$\begin{aligned} T_{avg} &= \frac{1}{\tau}\int_0^\tau T_e(t)dt \\ \text{with, } \tau &= \frac{60}{nN_r} \end{aligned} \quad (17)$$

Where n is the speed in the rotor (rpm), N_r is the number of poles in the rotor.

The torque ripple of the switched reluctance motor is expressed in Equation 18.

$$T_{\text{ripple}} = \frac{T_{\max} - T_{\min}}{T_{\text{avg}}} = \frac{\Delta T}{T_{\text{avg}}} \quad (18)$$

Where T_{max} is the maximum torque in the SRM; T_{min} is the minimum torque in the SRM.

The motion equation of the machine can be described by the Equation 19:

$$T_e - T_l = B\omega + j\frac{d\omega}{dt} \quad (19)$$

Where T_l is the load torque, B is the friction coefficient, and j is the inertia moment.

The Equation of the SRM efficiency is given as:

$$\eta = \frac{P_o}{P_{\text{in}}} = \frac{P_{\text{in}} - P_{\text{cu}} - P_{\text{core}}}{P_{\text{in}}} \quad (20)$$

Where P_o is the output power, P_{in} is the input power, P_{cu} is the copper loss P_{core} is the core loss.

V. RESULTS AND DISCUSSIONS

To evaluate the provided 12/8 and 10/8 SRMs and compare their performance, as showen in the first section include Tables 3 and 4 to compare the basic parameters and comparing the various losses through the bar charts illustrated in Figure 4. The results of the second section highlights a comparison of the electromagnetic analysis of the magnetic flux density, the vectorial distribution of magnetic flux density, and the magnetic intensity in Figures 5, 6 and 7, which contributes to a more precise analysis of the mechanical performance and an understanding of the electromagnetic behavior between the stator and rotor. The results in the last section present the various performance curves for both SRMs that include efficiency curves, torque, speed, Stranded losses, currents, voltages, and flux linkages.

Table 3: Evaluation of the 12/8 and 10/8 SRMs performance.

Parameters	12/8 SRM	10/8 SRM
Input DC Current (A):	23.7302	23.5383
Phase RMS Current (A):	36.7278	29.2256
Phase Current Density (A/mm^2):	11.095	7.00377
Iron-Core Loss (W):	0.0414556	0.207566
Output Power (W):	4962	4973.91
Input Power (W):	5220.63	5178.42
Efficiency (%):	95.0459	96.0508
Rated Speed (rpm):	9361.01	20904.7
Rated Torque (N.m):	5.0618	2.27209
Flux Linkage (Wb):	0.0559623	0.0255368
Maximum Output Power (W):	19203.7	22969.8

Source: Authors, (2025).

Both of the SRMs have roughly similar input DC current indicating comparable current consumption. The phase RMS current of the 12/8 SRM reaches 36.7278 versus 29.2256 A in the 10/8 SRM. The phase current density of the 12/8 SRM reaches 11.095 A/mm², while the 10/8 SRM reaches 7.00377 A/mm². This difference indicates that the 12/8 SRM consumes more power compared to the 10/8 SRM, which may affect the overall losses and increase the thermal and magnetic stress in the coils while contributing to significantly increasing the output torque.

The output power in the 12/8 SRM has 4962 W versus 4973.91 W in the 10/8 SRM. The input power in 12/8 SRM is 5220.63 W, and in 10/8 SRM is 5178.42 W. This data shows that 10/8 SRM has higher output power with lower input power and excels in producing the maximum power, which increases its efficiency as the 12/8 SRM efficiency reaches 95.0459%, while the 10/8 SRM efficiency reaches 96.0508%. The flux linkage data reveals that the 12/8 SRM has a higher flux of 0.0559623 Wb while the 10/8 SRM has 0.0255368 Wb.

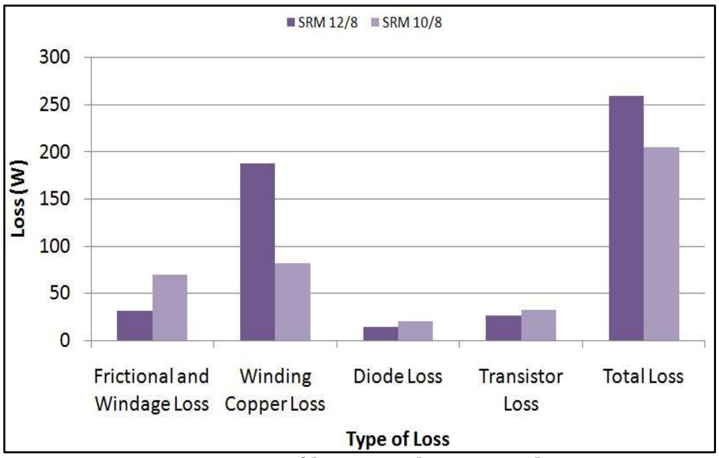

Figure 4: Comparison of losses in the 12/8 and 10/8 SRMs.
Source: Authors, (2025).

The frictional and windage loss in the 12/8 SRM is 31.2034 W, which is 55.2% less than the 10/8 SRM's 69.6824 W. This means that the 10/8 SRM has significantly higher frictional and windage loss, which reduces its dynamic efficiency. The 12/8 SRM significantly reduces iron core loss by about 80% to estimated 0.0414556 W, while in the 10/8 SRM it reaches 0.207566 W, which improves the behavior in magnetic conditions. The 12/8 SRM exhibits more winding copper loss of 187.693 W compared to the 10/8 SRM's 81.8344 W due to the increased number of stator poles, which may lead to overheating. The data illustrates that the 10/8 SRM has higher diode and transistor losses compared to the 12/8 SRM. This analysis shows that the 12/8 SRM is more efficient in terms of electronic components with a 32.5% improvement in diode loss compared to the 10/8 SRM. The 10/8 SRM has a total loss of 204.509 W, 20.9% less than the 12/8 SRM with 258.635 W, indicating a more power efficient functioning due to the consistency in the distribution of the number of poles.

Table 4: Estimation of the stator and rotor poles flux density and the winding of the 12/8 and 10/8 SRMs.

Parameters	12/8 SRM	10/8 SRM
Stator-Pole Flux Density (Tesla):	1.37232	1.04559
Stator-Yoke Flux Density (Tesla):	0.849767	0.775533
Rotor-Pole Flux Density (Tesla):	1.11211	1.01496
Rotor-Yoke Flux Density (Tesla):	0.2756	0.251524
Winding Resistance in Phase (ohm):	0.0463808	0.0191619
Winding Resistance at 20C (ohm):	0.038152	0.0157622
Winding Leakage Inductance (mH):	0.0275105	0.00980801

Source: Authors, (2025).

The flux density in the stator poles of the 12/8 SRM motor has 1.37232 Tesla, while in the 10/8 SRM it has 1.04559 Tesla. This difference shows that the 12/8 SRM achieves 31.1% higher magnetic density, which enhances its ability to generate greater torque and more efficient operation but also increases the possibility of magnetic saturation at high loads. As for the stator yoke flux density, it is 0.849767 Tesla in the 12/8 SRM compared to about 0.775533 Tesla in the 10/8 SRM. This difference indicates that the 12/8 SRM exhibits 9.5% higher density, which enhances the efficiency of magnetic usage and reduces magnetic losses.

For the rotor pole flux density, the 12/8 SRM has a 1.11211 Tesla, while the 10/8 SRM has a 1.01496 Tesla. This disparity reflects the preference of the 12/8 SRM, which enhances the motor's ability to produce torque and response to loads. the rotor yoke flux density reaches 0.2756 Tesla in the 12/8 SRM versus 0.251524 Tesla in the 10/8 SRM. This indicates that the 12/8 SRM has 9.6% greater density, which enhances behavior stabilization under various loads.

The winding resistance in phase of the 12/8 SRM has 0.0463808 ohms, while the 10/8 SRM has a lower resistance of 0.0191619 ohms. This indicates that the 12/8 SRM exhibits higher resistance in the windings leading to higher losses due to overheating. The 12/8 SRM exhibits higher resistance even when measuring the windings' resistance at 20°C. This difference reflects the 10/8 SRM's ability to reduce heating losses significantly, indicating its higher operational efficiency.

the 12/8 SRM has a higher winding leakage inductance value of 0.0275105 mH, which leads to power loss and response delay, while the 10/8 SRM shows a lower inductance of 0.00980801 mH. This enhances the motor response and minimizes losses due to the winding leakage inductance.

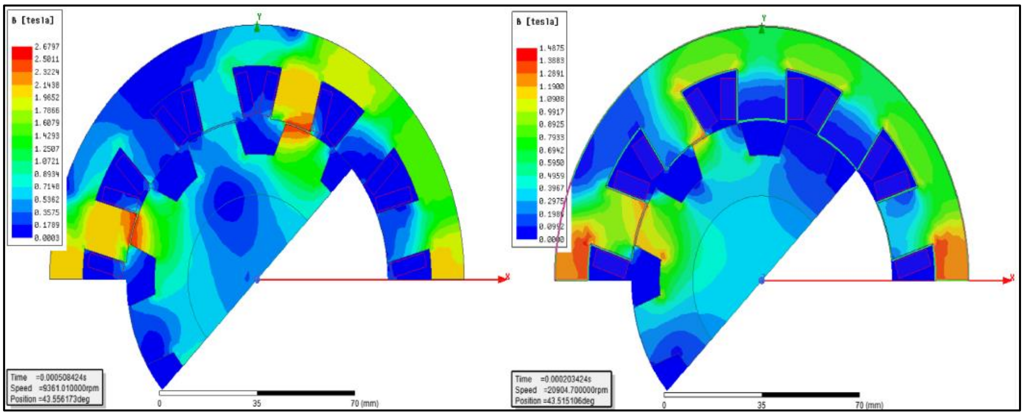

Figure 5: Variation of the SRMs Magnetic Flux Density.
Source: Authors, (2025).

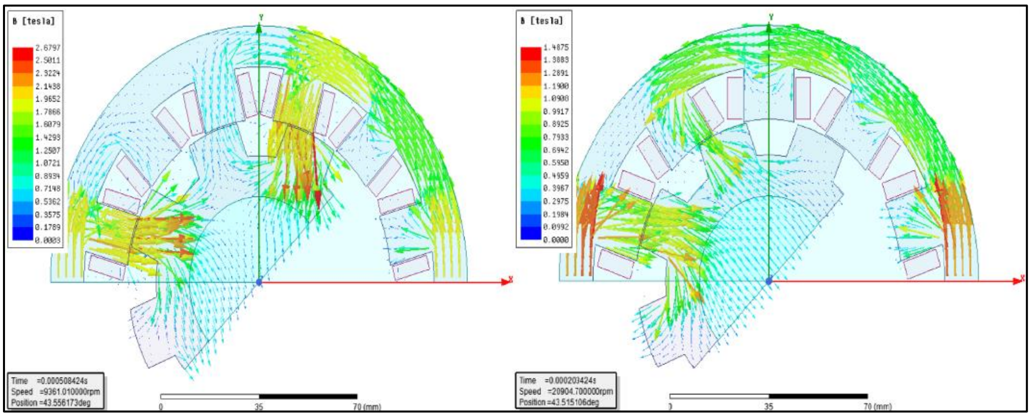

Figure 6: The SRMs vectorial distribution of magnetic flux density.
Source: Authors, (2025).

In Figures 5 and 6, the comparative analysis of the magnetic flux density at the same 43.5 degrees position indicates that the 12/8 SRM significantly outperforms the 10/8 SRM in terms of magnetic flux density and distribution, showing that the 12/8 SRM can generate a more powerful magnetic flux of 2. 6797 T by about 35% comparing to the 10/8 SRM's 1.4875 T. This indicates a higher performance in applications that require effective power conversion, efficient magnetization, and high torque, particularly at high loads. In contrast, the 10/8 SRM exhibits a lower performance due to the variability and irregularity of the flux distribution and its relatively low values.

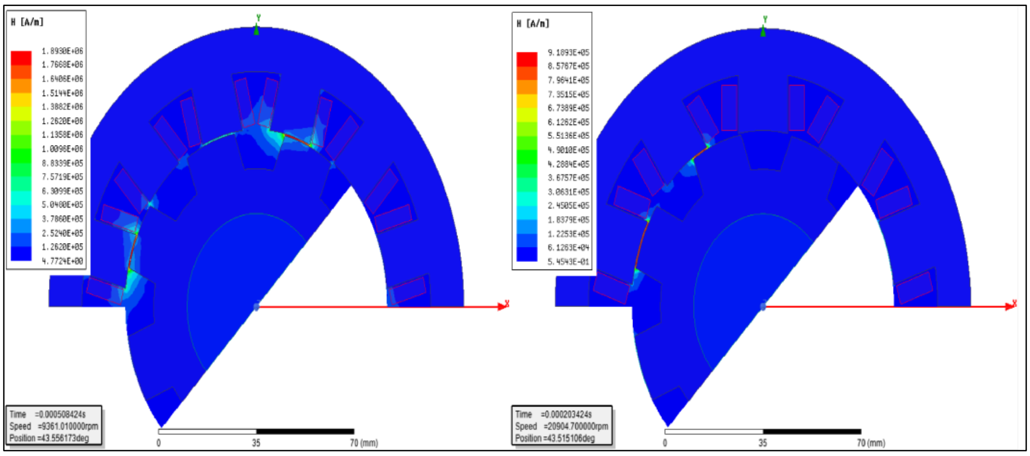

Figure 7: Variation of the SRMs Magnetic Intensity.
Source: Authors, (2025).

Figure 7 indicates the magnetic intensity distribution, showing that the 12/8 SRM is more balanced and uniform than the 10/8 SRM, with similar effective regions of maximum magnetic intensity. This reflects the stability of behavior and more efficient conversion of magnetic energy into mechanical energy. In contrast, the 10/8 SRM exhibits unbalanced and non-uniform magnetic intensity distribution, which can lead to reduced electromagnetic conversion efficiency and fluctuations in output torque.

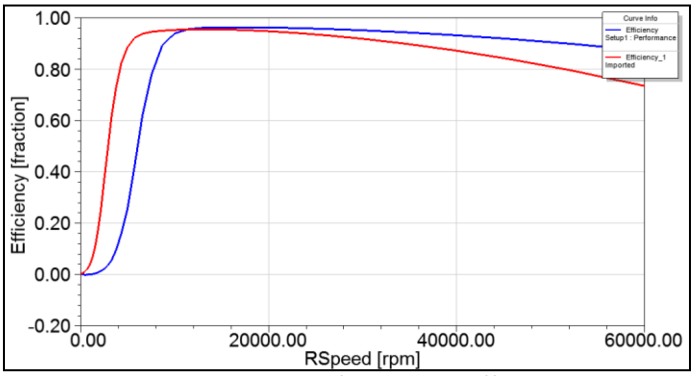

Figure 8: Variation of the SRMs Efficiency.
Source: Authors, (2025).

Figure 8 shows the variations in efficiency curves versus the speed for the 10/8 SRM shown in blue and the 12/8 SRM shown in red. The results indicate that the 12/8 SRM quickly reaches higher efficiency values initially at speeds below 12000 rpm compared to the 10/8 SRM. At speeds above 20000 rpm, the efficiency curve of the 12/8 SRM decreases gradually compared to the 10/8 SRM.

This decrease is due to the increasing dynamic losses and the losses due to eddy currents and electromagnetic interference which are affected by the design and number of stator poles while the 10/8 SRM retains its efficiency even as the speed increases making it more suitable for applications that require stable behavior at high rotational speeds.

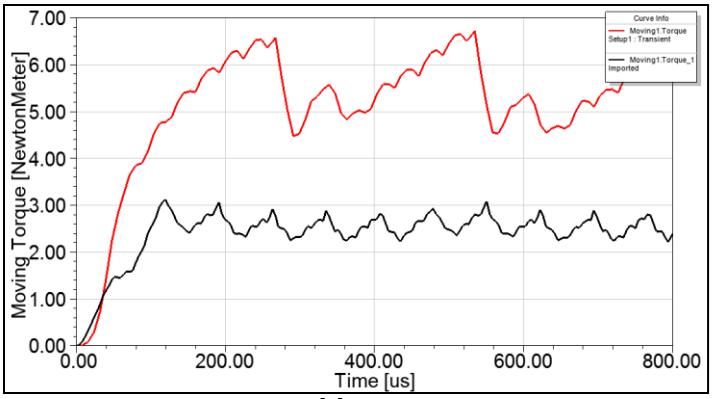

Figure 9: Variation of the SRMs Moving Torque.
Source: Authors, (2025).

The torque curves for both machines are shown in Figure 9. After increasing the number of stator poles of the SRMs, there is a 55.1% increase in average torque from 2.27 Nm to 5.06 Nm, indicating that the 12/8 SRM has improved dynamic behavior, increased power, and enhanced response to heavier loads, making it suitable for applications that require high torque and greater thrust.

However, the 12/8 SRM torque curve illustrated in blue exhibits a higher torque fluctuation compared to the 10/8 SRM, which is a result of increasing the number of stator poles, which leads to more complicated magnetic interactions and affects the performance stability. Note that in this case, the increase in stator poles was considered only without adjusting the other factors, but the fluctuation and ripple in torque of the 12/8 SRM can be reduced by improving the different aspects.

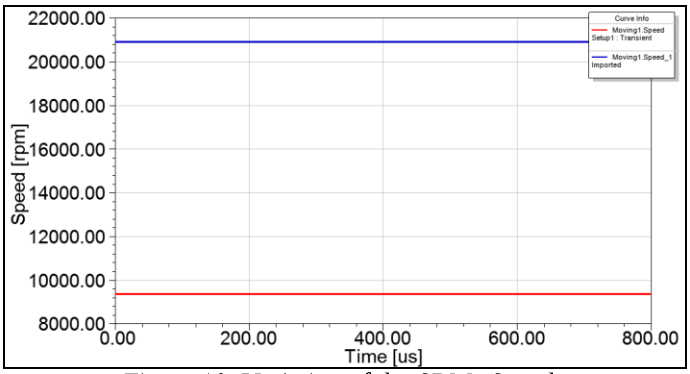

Figure 10: Variation of the SRMs Speed.
Source: Authors, (2025).

Based on the analysis of the speed curves as shown in Figure 10, the 10/8 SRM is more suitable for applications requiring high speeds and lower torque, with an estimated speed of 20904 rpm, which is 55.2% greater than the 12/8 SRM, which is suitable for applications requiring lower speeds and higher torque while maintaining control and stability, with an estimated speed of 9361 rpm. Although the 12/8 SRM provides higher torque, the emphasis on speed is a critical factor in many applications.

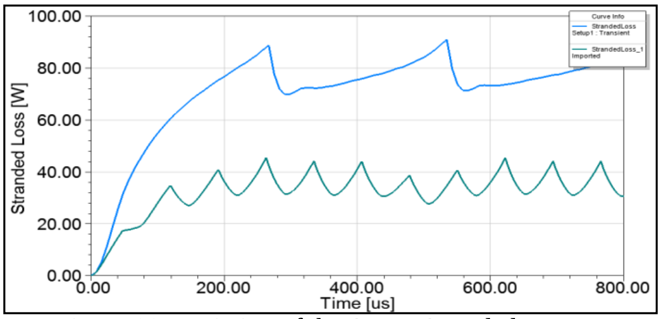

Figure 11: Variation of the SRMs Stranded Losses.
Source: Authors, (2025).

Figure 11 represents stranded loss curves where the 12/8 SRM shown in red exhibits a significantly higher stranded loss, up to 87.5 watts at extreme values. This indicates that more power is consumed to obtain a higher torque, which affects the overall efficiency. The stranded losses in the 10/8 SRM are noticeably lower with extreme values ranging around 37.5 watts. This illustrates the efficiency of the machine in terms of minimizing losses. This makes it a more suitable choice in applications that require low power consumption due to the consistency in the distribution of the poles as the stator poles are proportional to the rotor.

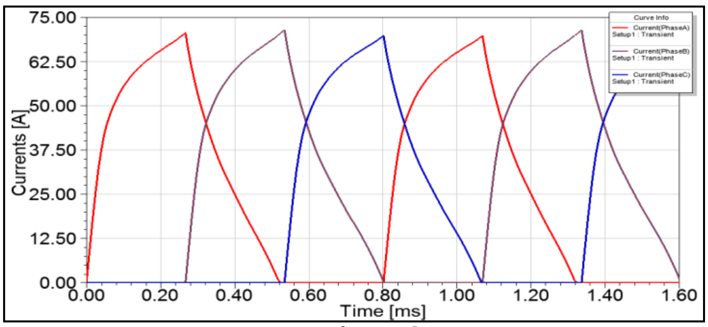

Figure 12: Variation of 12/8 the SRM Currents.
Source: Authors, (2025).

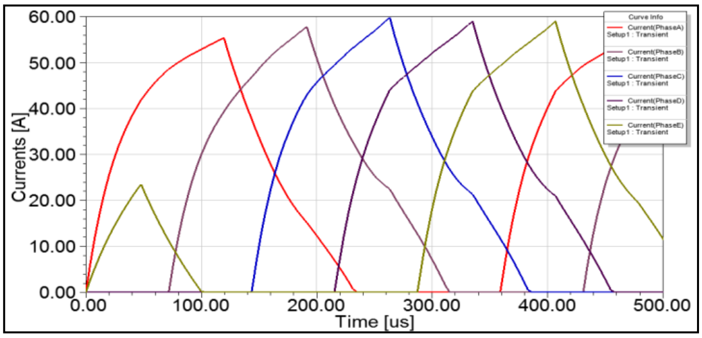

Figure 13: Variation of the 10/8 SRM Currents.
Source: Authors, (2025).

From Figures 12 and 13, the maximum current values in the 12/8 SRM reach about 75 A. While in the 10/8 SRM it reaches about 60 A. The maximum current in the 12/8 SRM appears to be about 25% more compared to the 10/8 SRM, reflecting the ability to produce greater torque and higher electrical power capacity in the phases. This means that the 12/8 SRM functions at lower speeds but provides a more steady current with distinct peaks and little overlap with other phases, indicating improved current distribution. Reducing the number of poles in the 10/8 SRM leads to interference between phases, which decreases the efficiency of the electromagnetic conversion and makes controlling the currents and power distribution between phases difficult and more complicated.

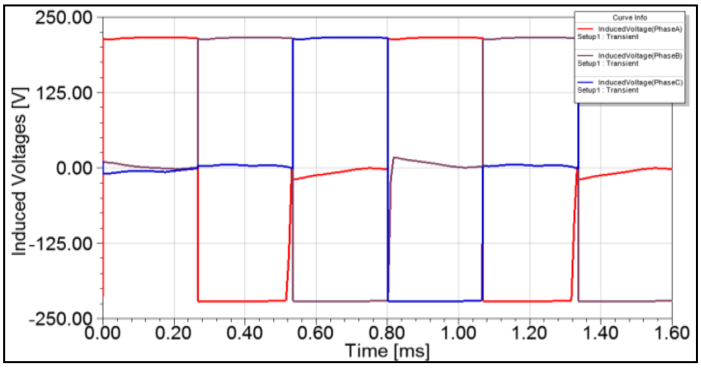

Figure 14: Variation of the 12/8 SRM Induced Voltages.
Source: Authors, (2025).

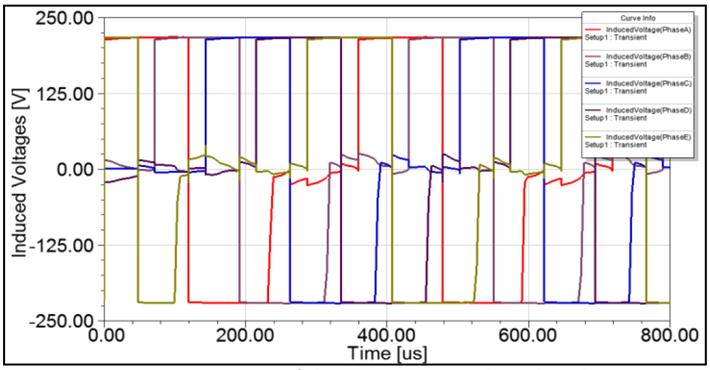

Figure 15: Variation of the10/8 SRM Induced Voltages.
Source: Authors, (2025).

Figures 14 and 15, represent the variation of the induced voltage vs the time. Both of the SRMs show an identical range of induced voltage values between 220V. Although the maximum values of the induced voltage are similar in both machines, the method of voltage generation and usage are significantly different between the two SRMs. The results show that the 12/8 SRM provides an easier and more stabilized control system due to the longer periods between voltage variations and the synchronization between the phases thus it is more appropriate in applications that require accuracy and stability in torque. On the other side, the 10/8 SRM requires advanced and complicated control techniques to handle the frequent interference and rapid variations in the induced voltage between the phases. Increasing the number of poles in the 12/8 SRM improves the synchronization and stabilization of the induced voltage across the phases, which facilitates torque control and aids in maintaining consistent dynamic behavior.

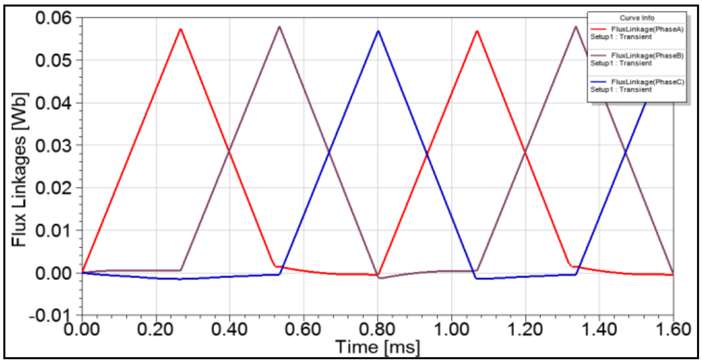

Figure 16: Variation of the 12/8 SRM Flux Linkages.
Source: Authors, (2025).

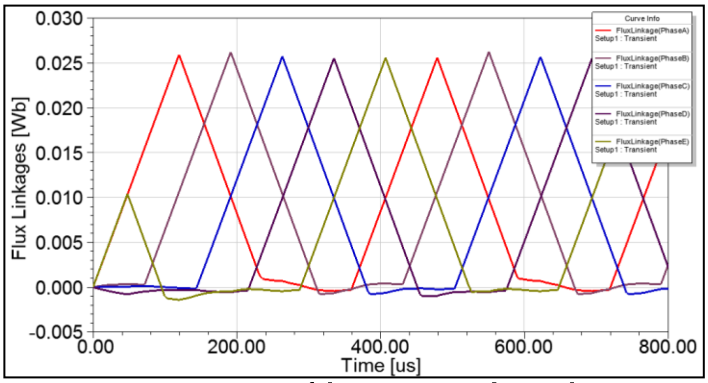

Figure 17: Variation of the 10/8 SRM Flux Linkages.
Source: Authors, (2025).

In Figures 16 and 17, it is shown that the flux linkage curves for both SRMs have a regular and repetitive form, reaching specific peaks of 0.057Wb at the 12/8 SRM and 0.026Wb at the 10/8 SRM and decreasing rapidly when the phase current is eliminated. It is clear from these results that the distribution of flux linkages is highly dependent on the number of poles and their design. In the 10/8 SRM, the peaks of the flux linkages are lower compared to the 12/8 SRM, with a greater overlap between the peaks. The response time is faster, indicating that the 12/8 SRM provides a more stabilized distribution of flux linkages with higher peaks and less overlap between the phases.

VI. CONCLUSIONS

This paper presents a comparative study of the designs of 12/8 and 10/8 SRMs featuring an effective design based on similar dimensions and operating conditions. Only the stator poles were changed to study its impact on efficiency, performance, and losses. The results show that increasing the number of poles in the stator varies the behavior of the current and its distribution between the phases and allows an increase in the maximum current values, leading to improved dynamic performance and torque stabilization. Reducing the number of poles in the 10/8 SRM leads to interference between phases, which leads to difficulty in maintaining torque stability and reduces the efficiency of the electromagnetic conversion. The 12/8 SRM has higher total losses, especially in copper losses, while the 10/8 SRM has higher of frictional and windage losses.

Electromagnetic analysis data shows that the 12/8 SRM has higher magnetic flux density and magnetic field strength, which enhances its ability to generate high torque, while the 10/8 SRM has higher efficiency in magnetic resistance and magnetic leakage, which makes it an appropriate choice in applications where high power efficiency is required. Both SRMs have distinct characteristics that make them suitable for different applications.

The choice between them depends on the specific application requirements in terms of speed, torque, efficiency, noise, and vibration. The 12/8 SRM can be used in applications that require high torque at low speeds and the 10/8 SRM in applications that require high speeds and low losses.

VII. AUTHOR'S CONTRIBUTION

Conceptualization: Layachi Chebabhi, Toufik tayeb Naas, Mohamed Zitouni.
Methodology: Layachi Chebabhi, Toufik tayeb Naas, Mohamed Zitouni.
Investigation: Layachi Chebabhi, Toufik tayeb Naas, Mohamed Zitouni.
Discussion of results: Layachi Chebabhi, Toufik tayeb Naas, Mohamed Zitouni.
Writing – Original Draft: Layachi Chebabhi, Toufik tayeb Naas, Mohamed Zitouni.
Writing – Review and Editing: Layachi Chebabhi, Toufik tayeb Naas, Mohamed Zitouni.
Resources: Layachi Chebabhi, Toufik tayeb Naas, Mohamed Zitouni.
Supervision: Author Two and Author Layachi Chebabhi, Toufik tayeb Naas, Mohamed Zitouni.
Approval of the final text: Author Layachi Chebabhi, Toufik tayeb Naas, Mohamed Zitouni.

VIII. REFERENCES

[1] Djaloul Karboua, Toufik Mebkhouta, Youcef Chouiha, Abdelkader Azzeddine Bengharbi, B. ouadeh Douara, and Belgacem Toual, "Enhancing Performance of Permanent Magnet Synchronous Motor Drives Through Hybrid Feedback Linearization and Sliding Mode Control," ITEGAM- Journal of Engineering and Technology for Industrial Applications (ITEGAM-JETIA), vol. 10, no. 49, pp. 178–186, Jan. 2024, doi: https://doi.org/10.5935/jetia.v10i49.1222.

[2] G. Challa and M. D. Reddy, "Acoustical Noise Mitigation in Slip Angle Controlled DTC of Open-End Winding Induction Motor Drive Using AISPWM Based Triple Randomization Scheme for EV Application," ITEGAM- Journal of Engineering and Technology for Industrial Applications (ITEGAM-JETIA), vol. 10, no. 49, pp. 202–210, Jan. 2024, doi: https://doi.org/10.5935/jetia.v10i49.1275.

[3] Sriramulu Naik Mudhavath, Kesana Gopikrishna, and A. Kumar, "DTC OF A 5 LEVEL MMC FED 3-Φ INDUCTION MOTOR WITH PI AND FLC USING CBAPOD PWM TECHNIQUE," ITEGAM- Journal of Engineering and Technology for Industrial Applications (ITEGAM-JETIA), vol. 10, no. 50, Jan. 2024, doi: https://doi.org/10.5935/jetia.v10i50.1295.

[4] S. Mafrici, V. Madonna, C. Maria Meano, K. Friis Hansen, and A. Tenconi, "Switched Reluctance Machine for Transportation and Eco-Design: A Life Cycle Assessment," IEEE Access, vol. 12, pp. 68334–68344, 2024, doi: https://doi.org/10.1109/access.2024.3400324.

[5] I. Mahmoud and Adel Khedher, "RETRACTED: Geometric Parameter Optimization of Switched Reluctance Machines for Renewable Energy Applications using Finite Element Analysis," Periodica Polytechnica Electrical Engineering and Computer Science, vol. 68, no. 2, pp. 178–192, Jan. 2024, doi: https://doi.org/10.3311/ppee.21747.

[6] A. Abdel-Aziz, M. Elgenedy, and B. Williams, "Review of Switched Reluctance Motor Converters and Torque Ripple Minimisation Techniques for Electric Vehicle Applications," Energies, vol. 17, no. 13, p. 3263, Jul. 2024, doi: https://doi.org/10.3390/en17133263.

[7] M. Omar, M. H. Bakr, and A. Emadi, "Advanced Design Optimization of Switched Reluctance Motors for Torque Improvement Using Supervised Learning Algorithm," IEEE Access, vol. 11, pp. 122057–122068, 2023, doi: https://doi.org/10.1109/access.2023.3328143.

[8] M. N. Kumar and R. Chidanandappa, "Particle swarm optimization technique for speed control and torque ripple minimization of switched reluctance motor using PID and FOPID controllers," International Journal of Information Technology, vol. 16, no. 2, pp. 1185–1201, Jan. 2024, doi: https://doi.org/10.1007/s41870-023-01656-2.

[9] D. M. Ismael and Thamir Hassan Atyia, "Comparative Evaluation of Speed Control Techniques for Switched Reluctance Motors in Industrial Applications," Engineering Research Express, Sep. 2024, doi: https://doi.org/10.1088/2631-8695/ad7d6b.

[10] P. Ren, J. Zhu, Y. Liu, Y. Zhao, and Z. Jing, "An Improved Model-Predictive Torque Control of Switched Reluctance Motor Based on Sector Adaptive Allocation Technology," IEEE Transactions on Power Electronics, vol. 39, no. 4, pp. 4567–4577, Jan. 2024, doi: https://doi.org/10.1109/tpel.2023.3349283.

[11] P. Saiteja and B. Ashok, "Experimental investigation of vibro-acoustic noise analysis in the switched reluctance motor through transient model-based multiphysics analysis for electric vehicles applications," Applied Acoustics, vol. 220, p. 109957, Mar. 2024, doi: https://doi.org/10.1016/j.apacoust.2024.109957.

[12] F. S. El-Faouri, Y. Cai, and A. Chiba, "Refinement of Analytical Current Waveform for Acoustic Noise Reduction in Switched Reluctance Motor," IEEE Open Journal of Industry Applications, vol. 5, pp. 325–337, 2024, doi: https://doi.org/10.1109/ojia.2024.3434668.

[13] Mouli Thirumalasetty and G. Narayanan, "Influence of Stator Winding Reconnection and Bipolar Excitation on the Performance Characteristics of Solid-Rotor Switched Reluctance Machine," IEEE Transactions on Industry Applications, vol. 60, no. 3, pp. 3773–3789, Jan. 2024, doi: https://doi.org/10.1109/tia.2024.3354225.

[14] H. Chen, F. Yu, W. Yan, and M. Orabi, "Calculation and Analysis of Eddy-Current Loss in Switched Reluctance Motor," IEEE Transactions on Applied Superconductivity, vol. 31, no. 8, pp. 1–4, Jun. 2021, doi: https://doi.org/10.1109/tasc.2021.3091068.

[15] Agus Adhi Nugroho, Muhammad Khosyi'in, Bustanul Arifin, Bhakti Yudho Suprapto, Muhamad Haddin, and Zainuddin Nawawi, "Load Effect on Switched Reluctance Motor Using Hysteresis Current and Voltage Control," pp. 59–63, Oct. 2021, doi: https://doi.org/10.23919/eecsi53397.2021.9624267.

[16] G. Sundari, R. Muniraj, and J. Shanmugapriyan, "Switched reluctance motor based water pumping system powered by solar using hybrid approach," Applied Energy, vol. 365, p. 123188, Jul. 2024, doi: https://doi.org/10.1016/j.apenergy.2024.123188.

[17] N. Priyadarshi, M. S. Bhaskar, Dhafer Almakhles, and F. Azam, "A New PV Fed High Gain Boost-Ćuk Converter Employed SRM Driven Water Pumping Scheme with IDEPSO MPPT," IEEE Transactions on Power Electronics, pp. 1–13, Jan. 2024, doi: https://doi.org/10.1109/tpel.2024.3459810.

[18] N. R. Patel, K. L. Mokariya, J. K. Chavda, and S. Patil, "A Novel Approach to the Design and Development of a C-Core Sandwich-Type Radial Field Switched Reluctance Motor with On-Shaft Implementation in EV Application," SAE International Journal of Electrified Vehicles, vol. 14, no. 1, Nov. 2024, doi: https://doi.org/10.4271/14-14-01-0007.

[19] Y. Zhu, W. Wei, J. Wang, and C. Xing, “Multi-objective optimization of switched reluctance motor driving electric vehicles based on vehicle operating condition,” Proceedings of the Institution of Mechanical Engineers Part D Journal of Automobile Engineering, Oct. 2024, doi: https://doi.org/10.1177/09544070241290073.

[20] M. A. Abdel, Hamdy Shatla, and M. Bahy, “Analysis of Slotted Tooth Switched Reluctance Motors for Electric Vehicle Applications,” Journal of Electrical and Computer Engineering, vol. 2024, no. 1, Jan. 2024, doi: https://doi.org/10.1155/2024/4493590.

[21] S. B. Shah, M. Khalid, and Berker Bilgin, “Design of a Switched Reluctance Motor for an Elevator Application,” pp. 1–6, Jun. 2024, doi: https://doi.org/10.1109/itec60657.2024.10598992.

[22] Augustine Mathu Gnaniah, E. Sehar, Appadurai Mangalaraj, and B. Mahadevan, “Thermal analysis of modified segmented switched reluctance motor with aluminium metal matrix composite fins used in cooling fan applications,” Matéria (Rio de Janeiro), vol. 29, no. 2, Jan. 2024, doi: https://doi.org/10.1590/1517-7076-rmat-2024-0075.

[23] M. Omar, M. Bakr, and A. Emadi, “Switched Reluctance Motor Design Optimization: A Framework for Effective Machine Learning Algorithm Selection and Evaluation,” 2024 IEEE Transportation Electrification Conference and Expo (ITEC), pp. 1–6, Jun. 2024, doi: https://doi.org/10.1109/itec60657.2024.10598839.

[24] A. L. Saleh and László Számel, “Improved Direct Instantaneous Torque Control Strategy of Switched Reluctance Motor based on Artificial Neural Network,” pp. 166–172, Jun. 2024, doi: https://doi.org/10.1109/gpecom61896.2024.10582580.

[25] W. Qiu, X. Zhao, A. Tyrrell, Suresh Perinpanayagam, S. Niu, and G. Wen, “Application of Artificial Intelligence-Based Technique in Electric Motors: A Review,” IEEE Transactions on Power Electronics, vol. 39, no. 10, pp. 13543–13568, Jun. 2024, doi: https://doi.org/10.1109/tpel.2024.3410958.

[26] L. Chebabhi, T. T. Naas, M. Zitouni, I. Ghibeche, and T. Benmessaoud, “Influence of choosing materials on 6/4 switched reluctance motor performance,” STUDIES IN ENGINEERING AND EXACT SCIENCES, vol. 5, no. 1, pp. 2391–2406, May 2024, doi: https://doi.org/10.54021/seesv5n1-118.

[27] M. R. Feyzi and Y. Ebrahimi, “Direct torque control of 5-Phase 10/8 switched reluctance motors,” DOAJ (DOAJ: Directory of Open Access Journals), Sep. 2009, [Online]. Available: https://doaj.org/article/d3442ec0953545e6abc67347a1d443f0

[28] M. R. Feyzi, Y. Ebrahimi, and M. Zeinali, “Direct torque control of 5-phase 10/8 switched reluctance motor by using fuzzy method,” International Journal of Engineering and Technology, vol. 1, no. 3, pp. 256–263, Jan. 2009, doi: 10.7763/ijet.2009.v1.48.

[29] N. Farah, M. H. N. Talib, J. Lazi, M. A. Ali, and Z. Ibrahim, “Multilevel Inverter Fed Switched Reluctance Motors (SRMs): 6/4, 8/6 and 10/8 SRM Geometric Types,” International Journal of Power Electronics and Drive Systems/International Journal of Electrical and Computer Engineering, vol. 8, no. 2, p. 584, Jun. 2017, doi: 10.11591/ijpeds.v8.i2.pp584-592.

[30] Krzysztof Bieńkowski et al., “Validated Analytical Model of 8/6 and 10/8 Switched Reluctance Motors,” Energies, vol. 15, no. 2, pp. 630–630, Jan. 2022, doi: https://doi.org/10.3390/en15020630.

[31] S. S. Chaware, M. F. A. R. Satarkar, and P. Kotwal, "10/8 Conventional Switched Reluctance Motor for Electric Vehicles," Journal of Emerging Technologies and Innovative Research (JETIR), vol. 11, no. 1, pp. 1–X, Jan. 2024.

[32] M. Chouitek, A. Chaouch, and B. Bekkouche, “COMPARISON OF THE VARIOUS CONTROLS OF THE SWITCHED RELUCTANCE MOTOR 12/8,” REVUE ROUMAINE DES SCIENCES TECHNIQUES — SÉRIE ÉLECTROTECHNIQUE ET ÉNERGÉTIQUE, vol. 68, no. 1, pp. 52–57, Apr. 2023, doi: 10.59277/rrst-ee.2023.68.1.9.

[33] H. Zhang, D.-H. Lee, C.-W. Lee, and J.-W. Ahn, “Design and analysis of a segmental rotor type 12/8 switched reluctance motor,” Journal of Power Electronics, vol. 14, no. 5, pp. 866–873, Sep. 2014, doi: 10.6113/jpe.2014.14.5.866.

[34] Ruchao Pupadubsin, Seubsuang Kachapornkul, Prapon Jitkreeyarn, Pakasit Somsiri, and Kanokvate Tungpimolrut, “Investigation of Torque Performance and Flux Reversal Reduction of a Three-Phase 12/8 Switched Reluctance Motor Based on Winding Arrangement,” Energies, vol. 15, no. 1, pp. 284–284, Jan. 2022, doi: https://doi.org/10.3390/en15010284.

[35] M. S. Rahman, G. F. Lukman, Pham Trung Hieu, K.-I. Jeong, and J.-W. Ahn, “Optimization and Characteristics Analysis of High Torque Density 12/8 Switched Reluctance Motor Using Metaheuristic Gray Wolf Optimization Algorithm,” Energies, vol. 14, no. 7, pp. 2013–2013, Apr. 2021, doi: https://doi.org/10.3390/en14072013.

[36] B. M. Dinh and D. H. Linh, “Torque Performances of Switched Reluctance Motor 12/8 By Rotor Pole Embrace Verification,” Mar. 2021, doi: https://doi.org/10.46254/an11.20210768.

[37] E. C. Abunike, G. D. Umoh, I. E. Nkan, and O. I. Okoro, “Investigating the Magnetic Characteristics of 12/8 Switched Reluctance Motor for Enhanced Starting Torque,” Nigerian Journal of Technological Development, vol. 18, no. 1, pp. 70–75, Jun. 2021, doi: https://doi.org/10.4314/njtd.v18i1.10.

[38] Sandeep Vuddanti, Vinod Karknalli, and Surender Reddy Salkuti, “Design and comparative analysis of three phase, four phase and six phase switched reluctance motor topologies for electrical vehicle propulsion,” Bulletin of Electrical Engineering and Informatics, vol. 10, no. 3, pp. 1495–1504, Jun. 2021, doi: https://doi.org/10.11591/eei.v10i3.3054.